

ATP-Dependent Allosteric DNA Enzymes

Matthew Levy and Andrew D. Ellington¹

Department of Chemistry and Biochemistry
Institute for Cell and Molecular Biology
University of Texas at Austin
Austin, Texas 78712

Summary

Effector-activated ribozymes that respond to small organic molecules have previously been generated by appending binding species (aptamers) to ribozymes. In order to determine if deoxyribozymes can similarly be activated by effector molecules, we have appended an anti-adenosine aptamer to a selected deoxyribozyme ligase. The resultant constructs are specifically activated by ATP. Optimization of the joining region resulted in ligases that are activated up to 460-fold by ATP. The selected deoxyribozyme catalyzes ligation largely via a templating mechanism. Effector activation is surprisingly achieved by suppression of the rate of the background, templated ligation reaction in the absence of the effector molecule, probably by misalignment of the oligonucleotide substrates. This novel allosteric mechanism has not previously been observed for nucleic-acid catalysts and is rare even in protein catalysts.

Introduction

The ability of RNA to catalyze reactions was first demonstrated by the discovery of natural ribozymes. However, to date no DNA enzymes have been found in nature, giving rise to the prejudice that RNA must be more catalytically “fit” than DNA [1–3]. Nonetheless, the ability of DNA to catalyze reactions has been amply demonstrated by the *in vitro* selection of multiple different deoxyribozymes, including cleavases that can hydrolyze either RNA or DNA [4–7], a DNA ligase [8], and DNA molecules that can phosphorylate [9] or cap [10] themselves.

It has also proven possible to design, engineer, and select ribozymes that are allosterically activated by effector molecules. By simply appending a known anti-adenosine aptamer to the hammerhead ribozyme, Tang and Breaker generated catalysts whose cleavage abilities were modulated by ATP [11]. Since then, a combination of rational design and *in vitro* selection techniques has been employed to generate allosteric ribozymes that are modulated by a variety of effector molecules ranging from small molecules such as ATP, FMN, and quinolone derivatives [11–14] to oligonucleotides [15–17] to proteins [18]. These approaches have been implemented with two different RNA “platforms,” the natural hammerhead ribozyme [11, 12] and a selected ligase ribozyme (L1) [13, 16, 18]. Between them, these ribo-

zymes exhibit a variety of allosteric mechanisms, including effector-induced steric interference [19], secondary-structure stabilization [16, 19, 20], antisense interactions [15–17], and a combination of both antisense interactions and structural stabilization as in a sequence-activated hammerhead “maxizyme” [20, 21]. However, in general the ligand-dependent stabilization of secondary and tertiary structure results in a concomitant stabilization of the catalytic domain and thus activation of catalysis [22].

While the design and selection of effector-dependent ribozymes is now well established, there has not been a great deal of complementary work with deoxyribozymes. Breaker and Roth were able to isolate RNA-cleaving deoxyribozymes that required the cofactor histidine [23]. In this instance, though, the cofactor appears to function as a general base in the cleavage reaction, rather than as an allosteric effector. More recently, Wang and Sen have used rational design to engineer an RNA-cleaving 10-23 deoxyribozyme [24] to require an oligonucleotide effector for activity [25]. The so-called “expansively regulated” deoxyribozyme catalyst forms a three-way helical junction with the oligonucleotide substrate and a novel effector oligonucleotide. The binding of the effector oligonucleotide enhances the binding of the substrate by effectively extending the substrate binding site of the deoxyribozyme. The effector oligonucleotide can thus be considered a cosubstrate of the reaction.

We have attempted to determine if the methods for generating allosteric ribozymes that respond to small organic effector molecules, such as ATP and FMN, could be successfully extended to deoxyribozymes. We have previously selected a deoxyribozyme ligase that catalyzes the formation of an unnatural internucleotide linkage [26, 27], starting from a pool that contained a 5' iodine and a substrate that contained 3' phosphorothioate, as originally described by Eric Kool and his coworkers [28]. A previously selected anti-adenosine, DNA aptamer that was known to undergo a significant conformational change upon ligand binding [29] was appended to the deoxyribozyme. As in previously designed allosteric ribozymes, the ligand-dependent conformational change is relayed to the catalytic core of the deoxyribozyme, and in optimized constructs ATP was found to modulate the rate of catalysis by up to 460-fold. However, the allosteric deoxyribozyme also employs a novel mechanism in that the conformation assumed in the absence of the effector actually depresses the rate of reaction below background, templated levels.

Results and Discussion

The Role of Templating in Catalysis

Deoxyribozyme ligases that could catalyze the attack of a 3' phosphorothioate on a 5' iodine residue were originally selected from a DNA pool that spanned 90 random sequence positions. We focused our initial ef-

¹Correspondence: andy.ellington@mail.utexas.edu

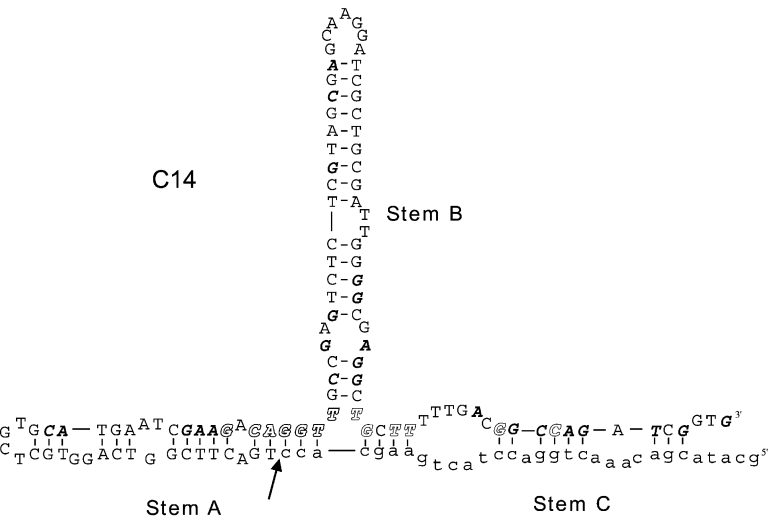


Figure 1. Putative Secondary Structure for Deoxyribozyme C14 with Substrate KSS6

The arrow indicates the ligation junction. KSS6 is shown in lowercase. Residues conserved in more than 75% of reselected clones are shown in bold; those conserved in more than 90% of reselected clones are shown in outlines.

forts on the previously characterized clone 14, which had a rate of 1.9 hr⁻¹ and showed more than a 400-fold rate enhancement over the unselected pool (Figure 1).

A series of deletion constructs were generated in order to better map the catalytic core of the deoxyribozyme ligase (Figure 2A). The predicted internal loops and nucleotide bulges proved to be relatively unimportant for catalysis. However, “stem B” contained several residues that were conserved after reselection (Figure 1). Consistent with our previous observations, these residues appeared to contribute to catalysis by an additional ~10-fold in a standard assay [26]. Overall, the deletion analyses were consistent with the secondary-structural hypothesis but, more importantly, yielded a minimal construct that could be readily synthesized. Opening “stem A” of the deoxyribozyme ligase resulted in a short, synthetic enzyme that could act on oligonucleotide substrates in *trans* (Figure 2B; mt14.wt). As was the case for the “*cis*” constructs, some aspect of stem B proved to be important for catalysis beyond simple templating function. We therefore initially began to examine residues in and near this stem. When residue T24 (Figure 3A, square) was changed from thymidine to cytidine, there was a 40-fold decrease in deoxyribozyme activity, consistent with the conservation of this residue after reselection (Figure 3B; mt14.1). More surprising, though, was the behavior of residue T11 (Figure 3A, circle), which paired with A41 of the substrate (Figure 3A, triangle). When T11 was mutated to a cytidine, the activity of the deoxyribozyme dropped by more than 750-fold. (Figure 3B; mt14.2). This residue appeared especially sensitive to mutation, and changes to A, G, or 5-methyl C all resulted in a substantial loss of activity (Figure 3B; mt14.3–5). Only the substitution to deoxyuridine retained activity (Figure 3B; mt14.6).

Although we have previously drawn the three-way junction, with a base pair between T11 and A41, as shown in Figures 1 and 3A (left), it was also possible that an alternate base pair could form between T24 and A41, leaving two unpaired T residues (Figure 3A, right). A series of mutations was designed to determine which residue, T11 (circle) or T24 (square), was nominally un-

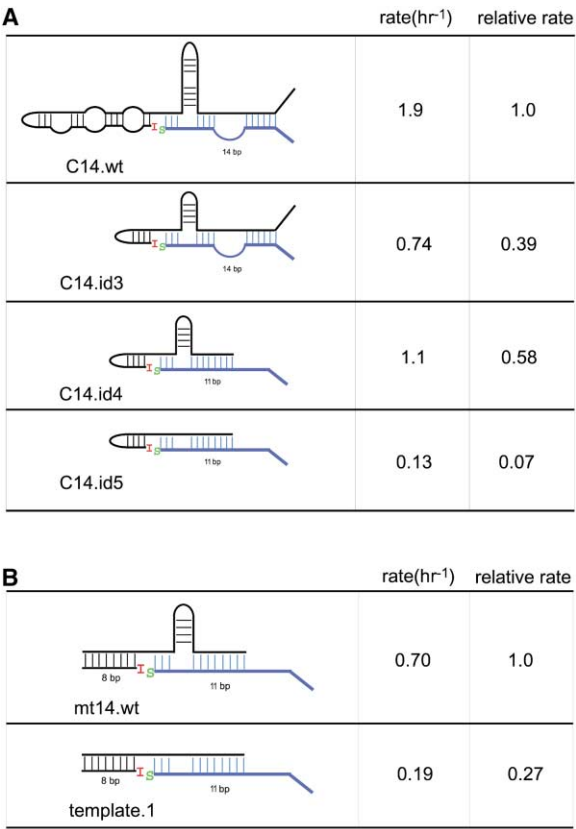


Figure 2. Ligation Rates of Deoxyribozyme Deletion Constructs

(A) Ligation rates of *cis* constructs. These deoxyribozymes ligate a single oligonucleotide substrate to themselves. Substrate #2 is shown in blue. The number of base pairs between the each construct and its substrate is schematically indicated. Initial rates are reported per hour, and relative rates are normalized with respect to the parental deoxyribozyme C14.

(B) Ligation rates of *trans* constructs. These deoxyribozymes catalyze the ligation of two oligonucleotide substrates. Initial rates are reported per hour, and relative rates are normalized with respect to mt14.wt.

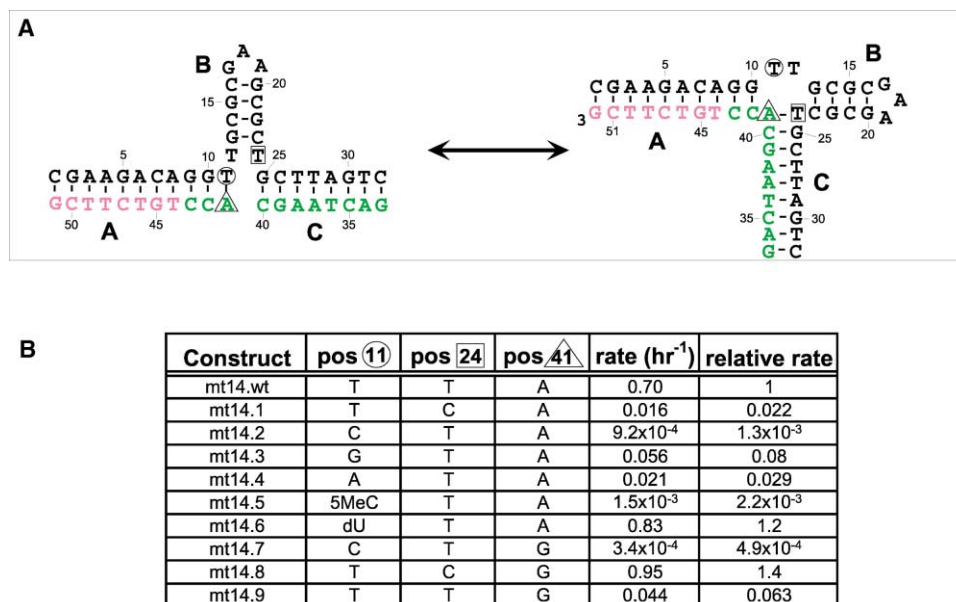


Figure 3. Mutational Analysis of the *Trans* Deoxyribozyme mt14.wt

(A) Two potential deoxyribozyme conformations. Iodinated substrate 5I.8.C14.m1 is shown in pink, and the eleven 3' nucleotides of substrate #2 are shown in green.

(B) Ligation rates of mutant deoxyribozymes. The identities of positions 11, 24, and 41 are explicitly shown. Initial rates are reported per hour, and relative rates are normalized with respect to mt14.wt.

paired in the deoxyribozyme secondary structure. When the originally predicted T11:A41 base pair was changed to a C:G base pair, the deoxyribozyme lost more than 2,000-fold in activity (Figure 3B; mt14.7). However, when the alternative T:A base pair between T24 and A41 was changed to a C:G base pair, the deoxyribozyme showed wild-type or better activity (Figure 3B; mt14.8). In general, mutations that included the predicted T24:A41 pairing were roughly as active as the predicted strength of the pairing, with Watson-Crick pairings showing greater activity than wobble pairings (compare constructs mt14.8 with 14.wt, 14.9 and 14.1).

Taken together, these results indicated that the alternative conformer shown in Figure 3A (right) is the more likely secondary structure for the deoxyribozyme ligase. In addition, these results strengthened the hypothesis that templating function and other catalytic mechanisms are intimately linked. Previous experiments with phosphorothioate-iodide ligation chemistry had established that mismatches between the iodinated oligonucleotide and its template resulted in a greater-than-100-fold loss in the rate of ligation [30]. However, although constructs mt14.wt and m14.7 should have been able to form the same number of base pairs with the template, they differed by more than 2,000-fold in activity. This was especially surprising given that the evolved catalyst was only 400-fold more active than the nascent pool. Thus, the mutation of a single base that was uninvolved in base pairing with the substrate misaligned the template to the point where catalysis was lower even than the background, templated reaction.

These results can to some extent be rationalized based on what is known about the three-dimensional structures and relative stabilities of three-way junctions.

It has been shown that the introduction of unpaired bases at the branch site of three-way junctions (e.g., residues T11 and T12) can have a stabilizing effect on these structures [31]. The introduction of such bulged residues has also been shown to reduce the flexibility of these three-way junctions [32] and to allow for the coaxial stacking of two of the three helices [33–35]. In the case of the oligonucleotide effector-dependent 10-23 deoxyribozyme designed by Wang and Sen, which includes a three-way helical junction, both the identity and position of two bulged adenosines at the junction were found to be important for activation [25]. Although we do not know the three-dimensional structure of our deoxyribozyme ligase, it is possible that the unpaired thymidine residues aid in the formation of an extended helix and hence in the alignment of the substrate oligonucleotide.

Designing Allosteric Deoxyribozymes

The finding that selected deoxyribozymes were sensitive to mutations in the TT bulge and that apparent misalignment of the template could drastically reduce ligase activity immediately suggested a method for designing allosteric deoxyribozymes. Breaker and his co-workers had previously found that the rate of the hammerhead ribozyme could be controlled by appending an anti-adenosine aptamer to the catalytic core [11]. Upon ligand binding, conformational changes in the aptamer were transmitted to the catalytic core. Depending upon the “communication module” that connected the aptamer and the catalytic core, the hammerhead ribozyme could either be activated or inhibited by the addition of ATP [11]. Communication modules can modulate ribozyme activity by various mechanisms, including

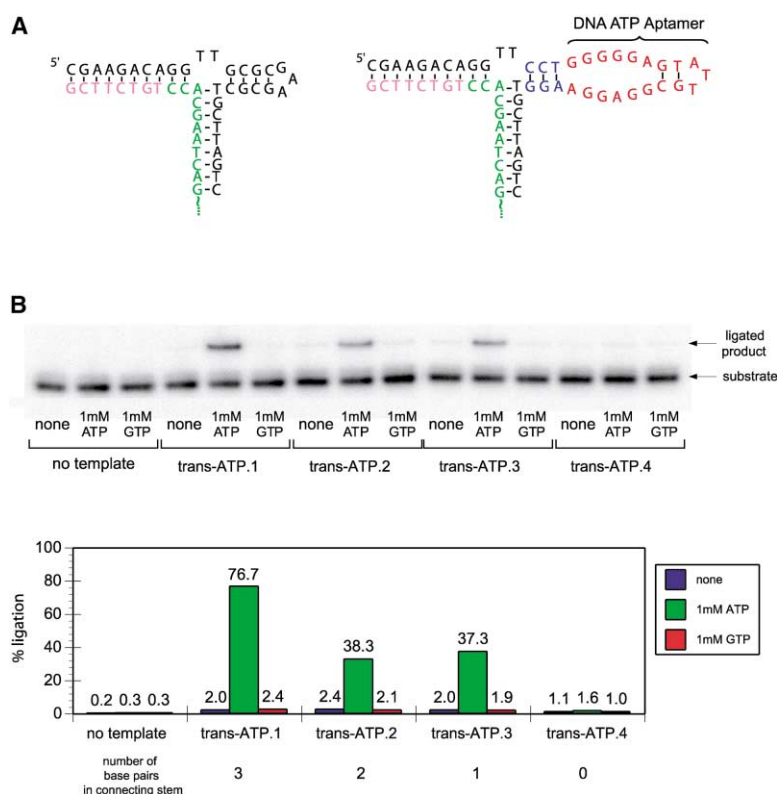


Figure 4. Rational Design of ATP-Dependent Deoxyribozyme Ligases

(A) Putative secondary structures of parental (mt14.wt, left) and effector-activated (KL.ATP.5, right) deoxyribozyme ligases. The iodinated substrate 5I.8.C14.m1 is shown in pink, and the eleven 3' nucleotides of substrate #2 are shown in green. The anti-adenosine aptamer is shown in red, and the joining region is in blue.

(B) Ligation assay for ATP-dependent deoxyribozyme ligases. The constructs trans-ATP.1, trans-ATP.2, trans-ATP.3 and trans-ATP.4 contained different numbers of base pairs in the joining region. Reactions were carried out with no effector, 1 mM ATP, or 1 mM GTP. The percent ligation values have been adjusted to reflect the fact that there was a 2-fold excess of labeled substrate in the reaction mixture.

both the relief or adoption of tertiary structural conformations that sterically hinder catalysis [19] and the alignment or misalignment of residues in a helical stem [36].

We similarly hoped to control the rate of the selected deoxyribozyme ligase by appending an anti-adenosine aptamer originally selected from a DNA pool by Hui-zenga and Szostak [37]. NMR structural analysis of the aptamer revealed a compact stem-bulge structure that could simultaneously bind two ATP ligands [29]. The aptamer underwent a conformational change in the absence and presence of ATP, with the ligand substantially stabilizing the paired stem. By appending the aptamer to one or more stems of the deoxyribozyme ligase, we hoped to engender ligand-dependent conformational changes that would align or misalign the template and to concomitantly control catalytic activity.

Initially, we designed several constructs in which the core DNA aptamer was appended to stem B of the minimized deoxyribozyme *trans* ligase. The joining region between the aptamer and the deoxyribozyme was systematically varied from 0 to 3 bp in length. The deoxyribozyme chimeras were assayed for their ability to join two oligonucleotide substrates either in the presence or absence of the cognate effector ATP and a non-cognate effector, GTP (Figures 4A and 4B). As expected, deoxyribozymes that had no appended aptamer showed no modulation of activity in the presence or absence of effectors (data not shown). However, three of the four designed constructs showed strong ATP dependence and showed no activation above background by GTP. Even a single base pair in the stem appeared to be sufficient to mediate ATP-dependent activation. Deoxyribozymes that contain stems greater

than 3 bp in length are constitutively active (data not shown). Stem length dependence in aptamer-mediated activation of catalysis has previously been observed with hammerhead ribozyme chimeras. Tang and Breaker systematically varied the stem length of the joining region between an anti-adenosine aptamer and the hammerhead ribozyme [19] and observed the optimal sequence length to be 4–5 bp. Similarly, Araki et al. varied the stem length between an anti-FMN aptamer and the hammerhead [38] and observed an optimal length of 3 bp.

Although these results appeared to flow from the design principles elaborated above, it was also possible that the activation phenomenon was somehow merely coincident with ATP rather than dependent upon it. For example, Breaker and his coworkers have recounted the selection of ribozymes that initially appeared to be effector dependent, but that merely refolded as a function of time or changes in solution pH [39]. To guard against such artifacts, we determined the time course of trans-ATP.1 activation (Figure 5A). Irrespective of the preincubation time, the deoxyribozyme remained relatively inactive until the addition of ATP; the initial rate of reaction increased 250-fold upon ATP addition (Figure 5B). The addition of ATP did not change the solution pH. The parent deoxyribozyme was not dependent on magnesium or other divalent metals [27], and the measured rates of ligation reactions did not change when Mg^{2+} concentration was increased from a 5-fold molar excess relative to ATP to a 50-fold excess. It is therefore unlikely that ATP-dependent changes in metal ion concentration affected catalysis.

As a final proof of allosteric activation, we examined

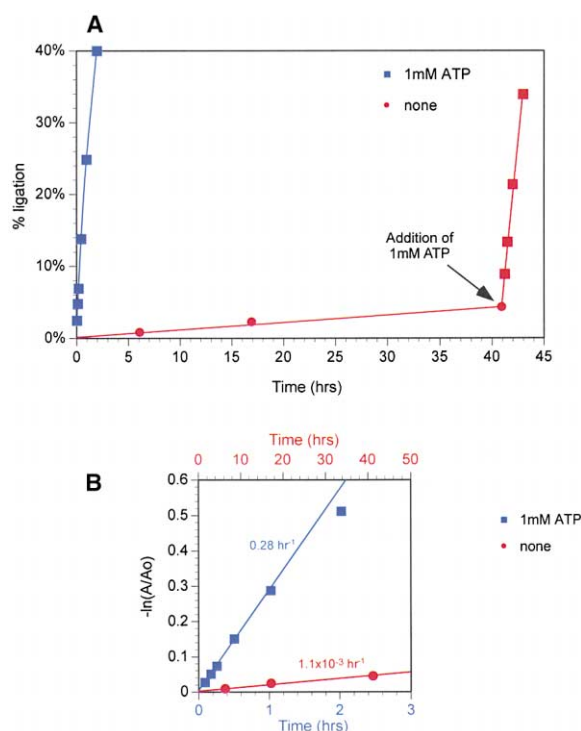


Figure 5. Kinetics of ATP Activation of Trans-ATP.1

(A) Extent of reaction as a function of time. The blue line indicates the extent of reaction when ATP is included in the reaction mixture. The red line indicates the initial extent of reaction when ATP is excluded from the reaction mixture; ATP is then added at 41 hr. (B) Initial rate determination for the reaction of trans-ATP.1 in the presence (blue) and absence (red) of 1 mM ATP. A is the amount of unreacted substrate, and A_0 is the amount of substrate at time 0. The rates of ligation are as indicated.

the effect of ATP concentration on the rate of ligation. The NMR structure had revealed that two ATP molecules were bound to the aptamer, and the symmetry of the binding sites suggested that they might bind cooperatively. Indeed, cooperative binding of ATP to the aptamer had previously been observed by our lab [40] as well as by others [41]. Consistent with these observations, the allosteric deoxyribozyme showed almost perfect cooperativity as a function of ATP concentration (Figure 6, red line); the data could not be fit if no cooperativity was assumed (Figure 6, blue line). The calculated Hill coefficient was 1.98. The equilibrium constant for ternary complex formation was $1.6 \times 10^{-7} \text{ M}^2$, and further analysis of the data with the Adair equation suggested that the first binding constant was on the order of 10 mM and the second was on the order of 10 μM . The initial K_d of the deoxyribozyme chimera is considerably larger than that of the aptamer alone (6 μM [37]). This increase in apparent K_d is similar to that observed with other effector-dependent ribozymes [13, 34, 36, 42] and may reflect the increase in free energy required to drive a conformational transition in the catalytic core of the deoxyribozyme. Interestingly, Jose et al. [43] have previously shown that different effectors acting on distinct allosteric sites can act cooperatively, whereas our results reveal a mechanism by which the same allosteric site can mediate cooperative induction.

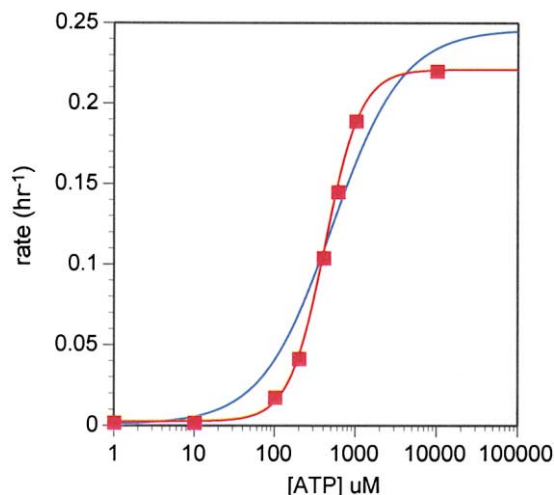


Figure 6. Activation of Trans-ATP.1 as a Function of ATP Concentration

Individual rates were determined by the best fit line of three initial time points, as described in the Experimental Procedures. The red line was generated by nonlinear regression analysis with the Hill equation, $v = v_0 + (V_{\max} x^n / K_{0.5}^n + x^n)$, where v is the rate, v_0 is the initial rate, V_{\max} is the maximum rate, $K_{0.5}$ is the equilibrium concentration at half saturation, and n is the Hill coefficient. The blue line represents the best fit line to the data if one assumes no cooperativity ($n = 1$).

Interestingly, the rate of ligation in the absence of the effector molecule is lower than the background, templated rate of ligation. In the presence of saturating amounts ATP, the rate of trans-ATP.1 is 0.22 hr^{-1} , only about 3-fold lower than that of the parental *trans* construct mt14.wt (Figure 2B, top, 0.70 hr^{-1}), and similar to the basal rate of template-directed ligation (Figure 2B, lower, 0.19 hr^{-1}). However, the initial rate of ligation of trans-ATP.1 in the absence of ATP is 0.0011 hr^{-1} , which is more than 100-fold slower (Figure 5B). The most consistent interpretation of these results is that in the absence of ATP the deoxyribozyme ligation substrates are misaligned on their template, whereas ATP binding engenders a conformational change that aligns the substrate oligonucleotides. This hypothesis is also consistent with the finding that single mutations in the deoxyribozyme could depress the rate of catalysis well below that of background reactions (Figure 3B). Of course, the observed templated rates are still faster (by at least 1000-fold) than untemplated reaction rates.

The depression of background reaction rates is a novel allosteric-activation mechanism that has previously not been observed for nucleic-acid catalysts. For example, Soukup and Breaker found that an FMN-activated hammerhead ribozyme still catalyzed phosphodiester bond cleavage approximately 100,000-fold more quickly than a corresponding background reaction [36]. Some protein catalysts also depress the rate of background reactions in order to direct reactivity. For example, carbamoyl phosphate synthetase and glutamine phosphoribosyl amidotransferase channel reactive intermediates to avoid hydrolysis [44]. However, in general, protein catalysts activate substrates for reaction and promote the formation of high-energy transition

states rather than depressing the ground state of reactions.

It is also interesting to compare the design scheme of our ATP effector deoxyribozyme with that of the oligonucleotide effector-dependent deoxyribozyme designed by Wang and Sen [25]. Although these two designs enable effector-dependent control of catalysis via two different mechanisms (effector-dependent template alignment versus effector-dependent substrate binding), both designs center on the formation and stabilization of three-way helical junction, suggesting that this may be a useful structure for the generation of other allosteric nucleic-acid catalysts.

Optimization of the Allosteric Deoxyribozyme Ligase

Previous selection experiments with aptamers [45, 46], nucleic-acid catalysts [13, 47], and effector-dependent ribozymes [12, 48] have revealed that initial constructs can be considerably improved by random mutagenesis and reselection. Therefore, in order to further optimize the activation of the deoxyribozyme ligase, we designed a pool in which the stem region joining the deoxyribozyme and aptamer domains was randomized. This strategy was similar to that employed by Soukup and Breaker with the hammerhead ribozyme [12] and by Robertson and Ellington with a ribozyme ligase [13]. The connecting region (Figure 7A) contained a random sequence mixture that was either 3 or 4 nucleotides in length. All possible combinations of sequences and lengths (102,400 variants) were represented in the library. The selection was conducted via a two-stage selection procedure employed previously in our laboratory and others [12, 13]. In the first round of selection, 10 pmol (approximately 6×10^7 copies of each sequence) of the single-stranded DNA (ssDNA) pool was incubated with the 5'-biotinylated substrate oligonucleotide in the absence of the effector molecule (ATP). This negative selection was allowed to proceed for 21 hr, at which point ligated species were removed from the population by binding to a streptavidin column. The effector (1 mM ATP) and additional substrate were added directly to the eluant, and a 1 hr positive selection was carried out. Ligated species were again captured on streptavidin agarose, they were selectively amplified, and the ssDNA pool was regenerated. Four rounds of selection and amplification were carried out under conditions of increasing stringency (Figure 7B).

Each round of selection was assayed for the ability to ligate the substrate #2 in the presence and absence of effector (Figure 7C). The first two rounds of selection showed an increase in effector-dependent ligation. However, whereas the third round of selection showed a 2-fold increase in the rate of reaction in the presence of effector, the rate of reaction in the absence of effector jumped almost 3-fold, reducing the overall level of activation. To further eliminate effector-independent catalysts, the negative selection in Round 4 was carried out for 19 days in the presence of an increased amount of substrate #2 (1.5 μM versus 0.15 μM). In addition, an alternative substrate (substrate #8), which shares the same eleven 3' terminal nucleotides as substrate #2 but

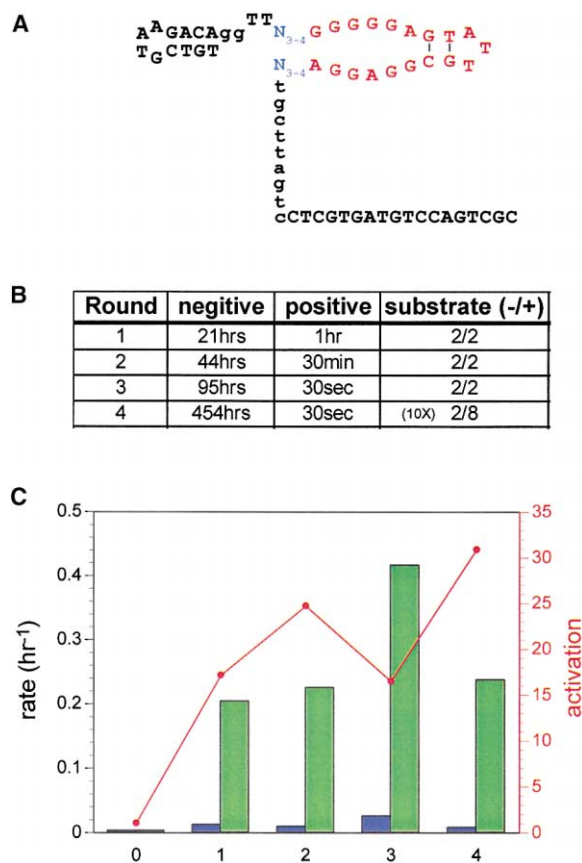


Figure 7. Optimization of Effector-Activated Deoxyribozymes

(A) Pool construction and design. The aptamer portion is shown in red, and the randomized stem region is shown in blue. The pool was designed to make a total of 11 base pairs (lowercase) with the 3' end of substrate #2.

(B) Conditions used during the course of the selection. The lengths of both negative and positive selection steps are indicated. Substrate #2 (denoted here as "2") was used for both the (–ATP) and (+ATP) selection steps except for the final round of selection, in which the alternative substrate #8 (denoted here as "8") was used in the (+) selection. The concentration of substrate was 0.15 μM for all rounds of the selection except for the negative selection step in the final round, in which it was increased to 1.5 μM (denoted here as 10X).

(C) Progress of the selection for ATP-dependent ligases. The initial rates of ligation of pools in the absence (blue) and presence (green) of 1 mM ATP are shown (scale on the left). The progression of the ratios of these rates is shown as a red line (scale on the right).

contains an alternative 5' tag sequence, was used for the positive selection. The use of an alternative substrate should have quelled the amplification of any ligated species that survived the negative selection. The increase in stringency in round 4 resulted in a more-than-30-fold increase in effector-dependent activation. Interestingly, the rate of reaction in the presence of effector after round 4 was almost 2-fold slower than for the previous round and similar to that observed in round 2, suggesting that those ligases that had the greatest effector dependence were not necessarily the fastest catalysts. Tradeoffs between kinetic parameters during evolutionary optimization have previously been a hallmark of protein evolution [49–51].













	cis			trans		
	activation	rate (hr ⁻¹) (+) ligand	(-) ligand	activation	rate (hr ⁻¹) (+) ligand	(-) ligand
cis-ATP.1 	55	0.46	0.0085	250 (trans -ATP.1)	0.28	0.00011
r4c1 	13*	0.15	0.011	-	-	-
r4c2 	340	0.26	0.0007	33	0.038	0.00012
r4c4 	1*	0.003	0.0046	-	-	-
r4c6 	51*	0.079	0.0015	26	0.051	0.002
r4c7 	460	0.32	0.0007	41	0.16	0.004
r4c8 	10*	0.41	0.04	-	-	-
r4c11 	110	0.13	0.0011	12	0.044	0.0038
r4c15 	60*	0.11	0.0018	-	-	-
r4c17 	340	0.67	0.0020	400	0.30	0.00075
r4c18 	270	0.28	0.0011	190	0.15	0.00078
r4c23 	160	0.31	0.0019	-	-	-

Figure 8. Activation Parameters of Optimized Deoxyribozymes

Putative secondary structures of the allosteric domains of optimized deoxyribozymes are shown on the left. The anti-adenosine aptamer is shown in red, and the selected residues in the joining region are shown in blue. Additional mutations are shown in black. Initial rates were determined by the best fit line through three initial data points, except where indicated (*; rates are based on a single data point).

Sequence analysis of the Round 4 deoxyribozymes revealed that multiple different clones remained in the population (Figure 8). No consensus sequence was observed, despite the fact that the initial population was relatively small. The diversity of the selected clones is perhaps not all that surprising when one considers that even simple, rationally designed, effector-dependent constructs show approximately 50-fold activation in *cis* (cis-ATP.1, Figure 8).

Detailed analysis of the initial rates of the selected catalysts are consistent with the hypothesis that the mechanism of activation primarily relies upon decreasing the rate of the background reaction, rather than increasing the rate of the catalyzed reaction. A wide range of activation parameters were observed, from al-

most no activation (r4c4) to more than 450-fold activation (r4c7). Reaction rates in the absence of effector were still significantly less than the background reaction rate for a linear template capable of making the same number of base pairs with a single substrate (Figure 2A; C14.id5, 0.13 hr⁻¹). Those clones that showed the most activation, such as r4c2, r4c7, r4c17, and r4c18, showed substantial decreases in the rate of reaction in the absence of effector relative to the parental construct and background reaction (C14.id4, C14.id5). The activated rates varied much less but, in general, were not greater than those of deoxyribozymes unperturbed by the addition of an aptamer (Figure 2A; C14.id4).

The best designed construct had shown 250-fold activation in *trans* but only 50-fold activation in *cis* (Figure

8, *cis*-ATP.1, compare left and right columns); therefore, hoping to see a further increase in activation (Figure 8, right), we assayed the selected variants for their ability to catalyze ligation reactions in *trans*. However, almost all of the clones tested (r4c2, r4c6, r4c11, and r4c23) showed a decrease in their effector-dependence in *trans*. The only exception was clone r4c17, which showed a slight increase in activation in *trans*. The decrease in effector-dependence was due in most cases to a decrease in the rate of reaction in the presence of the effector, but in some cases (e.g., r4c7) it was due to an increase in the basal ligation rate in the absence of effector. Overall, these results suggest that there is no direct correlation between *cis* and *trans* activation rates. This latter point is especially important because it may represent an inherent limitation on the direct selection methods currently used in most nucleic-acid catalyst selections [52–55]. That is, by selecting for single-turnover (*cis*) reactions, one may find it difficult or impossible to identify catalysts that are exceptional at multiple-turnover (*trans*) reactions.

Significance

Effector-dependent nucleic-acid enzymes or aptazymes can be adapted to function as biosensors (reviewed in [56]). For example, Breaker and his coworkers have generated an array of effector-activated hammerhead ribozymes and showed the specific and quantitative detection of a variety of ligands, from cobalt to cyclic mononucleotides [57]. Nucleic-acid ligases should prove to be even more versatile biosensors because they can potentially coimmobilize a wide variety of reporter molecules conjugated to oligonucleotide substrates [58]. In addition, the ligation products of nucleic-acid ligases are amplicons in their own right and can be detected with exquisite sensitivity by conventional amplification technologies. Aptazyme ligases therefore allow non-nucleic-acid analytes, such as ATP, to be transmogrified into readily detected nucleic acid [16]. However, all small-molecule effector-activated aptazymes to date have been ribozymes, which are inherently more difficult to chemically synthesize and more labile than deoxyribozymes. The demonstration that deoxyribozymes are amenable to many of the same methods used for the generation of allosteric ribozymes is an important step toward the continued generation of useful biosensors and biosensor arrays. More importantly, even though the parental deoxyribozyme showed little catalysis beyond templating, it nonetheless proved possible to engineer effector-dependence that was commensurate with some of the best designed hammerhead and ligase ribozymes [11, 13, 16, 36]. The misalignment of ligation substrates should prove to be a powerful general method for the development of aptazyme ligases. The normative conformation of the selected deoxyribozyme ligases will readily catalyze ligation, whereas there are multiple possible aptamer-induced conformations that will misalign substrates. The ease with which a small (32 nucleotide) core catalytic domain could be detached from its substrate also bodes well

for the development of new assay formats, such as the translocation of short oligonucleotides bearing reporters to short oligonucleotides immobilized on solid supports or chips.

Experimental Procedures

Sequences and Primers

The sequence of the C14 deoxyribozyme ligase is I-TGACTTCGGT CAGGTGCTCGTGCATGAATCGAAGACAGGTTGCCGAGTCTCTCG TAGCGAGCAAGGATCGCTCGATTGGGGCGAGGCTGCTTTTGA CGGCCAGATCGGTGCTCGTGATGTCCAGTCGC, where I-T denotes the 5'-iodinated thymine. Single-stranded DNA was generated from a double-stranded PCR product with the 5' primer 5I.22.90 (I-TGACTTCGGTCAAGGTCGTCGTCG) and the 3' primer 5B.18.90a (B-GCGACTGGACATCACGAG; where B is a 5' biotin), as previously described [26].

Deletion mutants C14.id3 (I-TGTCGTAAGACAGGTTGCGCGAAG CGCTGCTTTTACGCGCCAGATCGGTG); C14.id4 (I-TGTCGTAAGA CAGGTTGCGCGAAGCGCTGCTTAGTC); C14.id5 (I-TGTCGTAAGA CAGGTGCTTAGTC); *trans* constructs mt14.wt (CGAAGACAGGTT GCGCGAAGCGCTGCTTAGTC); template.1 (CGAAGACAGGTGCT TAGTC); mt14.1 (CGAAGACAGGTTGCGCGAAGCGCGCTTAGTC); mt14.2 (CGAAGACAGGCTGCGCGAAGCGCTTAGTC); substrates 5I.8.C14m1 (I-TGTCCTTCG); substrate #2 (TACATGTCTATCGATC TGACTAAGCACC-PS, where PS denotes a 3' phosphorothioate); 5B-substrate #2 (TACATGTCTATCGATCTGACTAAGCACC-PS); substrate #2.G41 (TACATGTCTATCGATCTGACTAAGCGCC-PS); 5B-substrate #8 (B-TGCTACTCATCTAGTCAGTCATCAAGACTAA GCACC); pool primers 5I.16.N3-4 (I-TGTCGTAAGACAGGTT); 5B.18.90.a (B-GCGACTGGACATCACGAG); and ATP constructs *trans*-ATP.1 (CGAAGACAGGTTCTGCGGAGTATTGCGGAGGAA GGTGCTTAGTC); *trans*-ATP.2 (CGAAGACAGGTTCTGCGGAGGTA TTGCGGAGGAAGTCTTAGTC); *trans*-ATP.3 (CGAAGACAGGTTT GGGGGAGTATTGCGGAGGAATGCTTAGTC); *trans*-ATP.4 (CGAA GACAGGTTGGGGAGTATTGCGGAGGATGCTTAGTC) were all synthesized in our laboratory on an Expedite 8909 DNA synthesizer (PE Biosystems, Foster City, California) via standard phosphoramidite chemistry. All synthesis reagents were purchased from Glen Research (Sterling, Virginia). The 3' phosphorothioates were synthesized on 3' phosphate-CPG by replacing the normal oxidizing reagent with the sulfurizing reagent thiosulfonate. Oligonucleotides containing 5' I-dT were deprotected in NH₄OH at room temperature for 24 hr; all other oligonucleotides were deprotected at 55°C for 16 hr. *Trans* constructs mt14.3 (CGAAGACAGGTTGCGCGAAGCG CTGCTTAGTC); mt14.4 (CGAAGACAGGATGCGCGAAGCGCTGCT TAGTC); mt14.5 (CGAAGACAGG5MedCTGCGCGAAGCGCTGCTTA GTC); and mt14.6 (CGAAGACAGGdUTGCGCGAAGCGCTGCTTA GTC) were purchased from IDT (Coralville, Iowa). All oligonucleotides were purified by denaturing PAGE in the presence of 7 M urea prior to use.

Pool Design and In Vitro Selection of Allosteric Deoxyribozyme Ligases

The ssDNA pool (TGTCGTAAGACAGGTTN₃₋₄GGGGGAGTATTGCG GAGGAN₃₋₄TGCTTAGTCCTCGTGATGTCCAGTCGC; aptamer domain underlined, N = A, G, C or T) was synthesized using an ABI 394 DNA synthesizer as previously described [13]. Positions denoted N were generated by equimolar mixing of phosphoramidites by the synthesizer. The pool was synthesized with a 5'-I-dT moiety. After deprotection and gel purification the ssDNA was used directly for selection.

The selection protocol for effector-dependent deoxyribozyme ligases was derived from the original selection protocol for deoxyribozyme ligases [27] and selection protocols for effector-dependent ribozyme ligases [13, 18]. At root, the selection protocol relies on coupled negative and positive selection steps. In the first round, 10 pmol of the pool (final concentration, 0.1 μM) was incubated with 15 pmol of substrate 5B-substrate #2 in selection buffer (500 mM NaCl, 50 mM Tris [pH 7.4], 10 mM MgCl₂, and 500 μM DTT) in the absence of effector for 21 hr. Ligated species were then removed from the population by passage of the reaction through a column

of streptavidin agarose (Sigma, St. Louis, Missouri). The eluant was replenished with 15 pmol of substrate 5B.KSS2 and 100 pmol of ATP (final concentration, 1 mM) and incubated at 25°C for 1 hr. This positive-selection step was stopped by the addition of 1 ml of stop buffer (7 M urea, 300 mM sodium acetate [pH 5.2]). Ligated species were captured on streptavidin agarose in the presence of the stop buffer. Ligated species were selectively amplified directly from the resin with a selective 5' primer that contained the same sequence as the substrate used in the reaction and a common 3' primer. The selective PCR product served as a template for regenerative PCR with a nested 5' primer containing iodine and a 3' primer containing biotin. Single-stranded DNA was isolated and used for additional rounds of selection and amplification as previously described [27]. Selection stringency was increased by increasing incubation times in the absence of effector and decreasing incubation times in the presence of effector (Figure 7B). For round 4, the concentration of the substrate #2 in the negative selection was increased from 0.15 μ M to 1.5 μ M. In addition, to avoid contamination by ligated species from previous rounds of selection, we employed an alternative substrate, 5B-substrate #8, in the positive selection step in round 4. This substrate shares the same eleven 3'-terminal nucleotides as 5B-substrate #2 but contains a different 5' tag sequence.

Cloning Deoxyribozymes

PCR products from round 4 were cloned with the Topo TA cloning kit (Invitrogen, Carlsbad, California). The dideoxy method was used for sequencing, and sequences were acquired on a CEQ 2000XL automated sequencer (Beckman Coulter, Fullerton, California).

Ligation Assays

Ligation assays for all *cis*-acting deoxyribozymes (including deletion constructs, selection rounds 0 through 4, and isolated effector-dependent clones) were carried out at 25°C with trace (\sim nM) amounts of 3' end-radiolabeled ssDNA and 0.15 μ M substrate, as previously described [26]. The ssDNA was 3' end labeled with terminal deoxynucleotide transferase (Gibco BRL, Gaithersburg, Maryland) and dideoxyadenosine 5'-(α - 32 P)-triphosphate (Amersham Pharmacia Biotech, Piscataway, New Jersey). The ssDNA was heat-denatured at 70°C and cooled to 25°C in selection buffer prior to the addition of DTT-treated substrates and effector. The final concentration of DTT in reactions was 500 μ M. Reactions were initiated by the addition of effector (10–100 mM ATP [pH 7] or water in the case of mock reactions) and substrates.

Trans ligation reactions were carried out in selection buffer at 25°C with 0.5 μ M ssDNA constructs and 1.0 μ M 5l.8.C14m1 with substrate #2. Constructs mt14.7, 14.8, and 14.9 are the same as constructs mt14.2, 14.1, and 14.wt. These reactions were carried out with substrate #2.G41. Iodinated 5l.8.C14m1 was 3' end labeled as described above. All reactions were carried out in selection buffer except for those in which the activity of KL.ATP.5 was measured as a function of ATP concentration; these reactions contained 50 mM MgCl₂ rather than 10 mM MgCl₂.

All reactions were terminated by the addition of 95% formamide gel-loading buffer. Ligated and unligated species were separated on denaturing 8% acrylamide gels containing 7 M urea and quantitated on a Phosphorimager (Molecular Dynamics, Sunnyvale, California).

Ligation reactions were initially linear as a function of time, and pseudo-first-order rates were determined by the best fit line through three points ($<10\%$ reaction) except where indicated. Ligation reactions typically proceeded to $>70\%$ reaction. Unreacted species may have lost the iodine leaving group or folded into an unreactive conformation.

None of the *trans* constructs were capable of performing multiple-turnover reactions. Reaction rates were therefore calculated with the assumption of single-turnover, pseudo-first-order kinetics. Rate analyses on c14.Trxn.4 were carried out four times, and the calculated rates differed by $\pm \sim 20\%$.

The cooperativity of effector dependence was determined by nonlinear regression with the program SigmaPlot (SPSS Science, Chicago, Illinois). Data was fit with the Hill equation:

$$v = v_0 + (V_{\max} x^n / K_{0.5}^n + x^n)$$

where v is the rate, v_0 is the initial rate, V_{\max} is the maximum rate, $K_{0.5}$ is the equilibrium concentration at half maximal saturation, and n is the Hill coefficient. Calculated values were as follows: $v_0 = 0.002 \pm 0.002 \text{ hr}^{-1}$, $V_{\max} = 0.22 \pm 0.003 \text{ hr}^{-1}$, $K_{0.5} = 430 \pm 10.0 \text{ M}^2$, $n = 1.98 \pm 0.07$. Individual binding constants were estimated by nonlinear regression with the Adair equation for two binding sites:

$$v = \frac{\left(\frac{[s]}{k_1} + \frac{2 \times [s]^2}{k_1 k_2} \right)}{2 \times \left(1 + \frac{[s]}{k_1} + \frac{[s]^2}{k_1 k_2} \right)} \times V_{\max} + v_0$$

where k_1 and k_2 are the binding constants, s is the concentration of effector, V_{\max} is the maximum rate, and v_0 is the initial rate. The calculated values were as follows: $k_1 = 13 \pm 24 \text{ mM}$, $k_2 = 14 \pm 29 \text{ } \mu\text{M}$, $V_{\max} = 0.22 \pm 0.003 \text{ hr}^{-1}$, and $v_0 = 0.002 \pm 0.002 \text{ hr}^{-1}$.

Acknowledgments

We thank Kenneth A. Johnson for a discussion on allostery. This work was supported by grant NCC2-1055 from the National Aeronautics and Space Administration (NASA) Astrobiology Institute, a research grant from the Arnold and Mabel Beckman Foundation, and National Institutes of Health grant 1R01GM61789-01A1.

Received: November 16, 2001

Revised: January 7, 2002

Accepted: January 22, 2002

References

- Cate, J.H., Gooding, A.R., Podell, E., Zhou, K., Golden, B.L., Kundrot, C.E., Cech, T.R., and Doudna, J.A. (1996). Crystal structure of a group I ribozyme domain: principles of RNA packing. *Science* 273, 1678–1685.
- Sigurdsson, S.T., and Eckstein, F. (1995). Structure-function relationships of hammerhead ribozymes: from understanding to applications. *Trends Biotechnol.* 13, 286–289.
- Li, Y., and Breaker, R.R. (1999). Deoxyribozymes: new players in the ancient game of biocatalysis. *Curr. Opin. Struct. Biol.* 9, 315–323.
- Breaker, R.R., and Joyce, G.F. (1994). A DNA enzyme that cleaves RNA. *Chem. Biol.* 1, 223–229.
- Carmi, N., Shultz, L.A., and Breaker, R.R. (1996). In vitro selection of self-cleaving DNAs. *Chem. Biol.* 3, 1039–1046.
- Geyer, C.R., and Sen, D. (1997). Evidence for the metal-cofactor independence of an RNA phosphodiester-cleaving DNA enzyme. *Chem. Biol.* 4, 579–593.
- Faulhammer, D., and Famulok, M. (1997). Characterization and divalent metal-ion dependence of in vitro selected deoxyribozymes which cleave DNA/RNA chimeric oligonucleotides. *J. Mol. Biol.* 269, 188–202.
- Cuenoud, B., and Szostak, J.W. (1995). A DNA metalloenzyme with DNA ligase activity. *Nature* 375, 611–614.
- Li, Y., and Breaker, R.R. (1999). Phosphorylating DNA with DNA. *Proc. Natl. Acad. Sci. USA* 96, 2746–2751.
- Li, Y., Liu, Y., and Breaker, R.R. (2000). Capping DNA with DNA. *Biochemistry* 39, 3106–3114.
- Tang, J., and Breaker, R.R. (1997). Rational design of allosteric ribozymes. *Chem. Biol.* 4, 453–459.
- Soukup, G.A., and Breaker, R.R. (1999). Engineering precision RNA molecular switches. *Proc. Natl. Acad. Sci. USA* 96, 3584–3589.
- Robertson, M.P., and Ellington, A.D. (2000). Design and optimization of effector-activated ribozyme ligases. *Nucleic Acids Res.* 28, 1751–1759.
- Piganeau, N., Thuillier, V., and Famulok, M. (2001). In vitro Selection of Allosteric Ribozymes: Theory and Experimental Validation. *J. Mol. Biol.* 312, 885–898.
- Porta, H., and Lizardi, P.M. (1995). An allosteric hammerhead ribozyme. *Biotechnology* 13, 161–164.
- Robertson, M.P., and Ellington, A.D. (1999). In vitro selection of

- an allosteric ribozyme that transduces analytes to amplicons. *Nat. Biotechnol.* **17**, 62–66.
17. Komatsu, Y., Yamashita, S., Kazama, N., Nobuoka, K., and Oh-tsuka, E. (2000). Construction of new ribozymes requiring short regulator oligonucleotides as a cofactor. *J. Mol. Biol.* **299**, 1231–1243.
18. Robertson, M.P., and Ellington, A.D. (2001). In vitro selection of nucleoprotein enzymes. *Nat. Biotechnol.* **19**, 650–655.
19. Tang, J., and Breaker, R.R. (1998). Mechanism for allosteric inhibition of an ATP-sensitive ribozyme. *Nucleic Acids Res.* **26**, 4214–4221.
20. Zhou, J.M., Nakamatsu, Y., Kuwabara, T., Warashina, M., Tanaka, Y., Yoshinari, K., and Taira, K. (2000). Chemical and enzymatic probing of effector-mediated changes in the conformation of a maxizyme. *J. Inorg. Biochem.* **78**, 261–268.
21. Kuwabara, T., Warashina, M., Tanabe, T., Tani, K., Asano, S., and Taira, K. (1998). A novel allosterically trans-activated ribozyme, the maxizyme, with exceptional specificity in vitro and in vivo. *Mol. Cell* **2**, 617–627.
22. Soukup, G.A., and Breaker, R.R. (1999). Nucleic acid molecular switches. *Trends Biotechnol.* **17**, 469–476.
23. Roth, A., and Breaker, R.R. (1998). An amino acid as a cofactor for a catalytic polynucleotide. *Proc. Natl. Acad. Sci. USA* **95**, 6027–6031.
24. Santoro, S.W., and Joyce, G.F. (1997). A general purpose RNA-cleaving DNA enzyme. *Proc. Natl. Acad. Sci. USA* **94**, 4262–4266.
25. Wang, D.Y., and Sen, D. (2001). A novel mode of regulation of an RNA-cleaving DNAzyme by effectors that bind to both enzyme and substrate. *J. Mol. Biol.* **310**, 723–734.
26. Levy, M., and Ellington, A.D. (2002). In vitro selection of a deoxy-ribozyme that can utilize multiple substrates. *J. Mol. Evol.* **54**, 180–190.
27. Levy, M., and Ellington, A.D. (2001). Selection of deoxyribozyme ligases that catalyze the formation of an unnatural internucleotide linkage. *Bioorg. Med. Chem.* **9**, 2581–2587.
28. Xu, Y., and Kool, E.T. (1997). A novel 5'-iodonucleoside allows efficient nonenzymic ligation of single-stranded and duplex DNAs. *Tetrahedron Lett.* **38**, 5595–5598.
29. Lin, C.H., and Patel, D.J. (1997). Structural basis of DNA folding and recognition in an AMP-DNA aptamer complex: distinct architectures but common recognition motifs for DNA and RNA aptamers complexed to AMP. *Chem. Biol.* **4**, 817–832.
30. Xu, Y., and Kool, E.T. (1999). High sequence fidelity in a non-enzymatic DNA autoligation reaction. *Nucleic Acids Res.* **27**, 875–881.
31. Leontis, N.B., Kwok, W., and Newman, J.S. (1991). Stability and structure of three-way DNA junctions containing unpaired nucleotides. *Nucleic Acids Res.* **19**, 759–766.
32. Yang, M., and Millar, D.P. (1996). Conformational flexibility of three-way DNA junctions containing unpaired nucleotides. *Biochemistry* **35**, 7959–7967.
33. van Buuren, B.N., Overmars, F.J., Ippel, J.H., Altona, C., and Wijmenga, S.S. (2000). Solution structure of a DNA three-way junction containing two unpaired thymidine bases. Identification of sequence features that decide conformer selection. *J. Mol. Biol.* **304**, 371–383.
34. Rosen, M.A., and Patel, D.J. (1993). Structural features of a three-stranded DNA junction containing a C–C junctional bulge. *Biochemistry* **32**, 6576–6587.
35. Rosen, M.A., and Patel, D.J. (1993). Conformational differences between bulged pyrimidines (C–C) and purines (A–A, I–I) at the branch point of three-stranded DNA junctions. *Biochemistry* **32**, 6563–6575.
36. Soukup, G.A., and Breaker, R.R. (1999). Design of allosteric hammerhead ribozymes activated by ligand-induced structure stabilization. *Struct. Fold. Des.* **7**, 783–791.
37. Huizenga, D.E., and Szostak, J.W. (1995). A DNA aptamer that binds adenosine and ATP. *Biochemistry* **34**, 656–665.
38. Araki, M., Okuno, Y., Hara, Y., and Sugiura, Y. (1998). Allosteric regulation of a ribozyme activity through ligand-induced conformational change. *Nucleic Acids Res.* **26**, 3379–3384.
39. Koizumi, M., Soukup, G.A., Kerr, J.N., and Breaker, R.R. (1999). Allosteric selection of ribozymes that respond to the second messengers cGMP and cAMP. *Nat. Struct. Biol.* **6**, 1062–1071.
40. Jhaveri, S.D., Kirby, R., Conrad, R., Maglott, E.J., Bowser, M., Kennedy, R.T., Glick, G., and Ellington, A.D. (2000). Designed signaling aptamers that transduce molecular recognition to changes in fluorescence intensity. *J. Am. Chem. Soc.* **122**, 2469–2473.
41. Battersby, T.R., Ang, D.N., Burgstaller, P., Jurczyk, S.C., Bowser, M.T., Buchanan, D.D., Kennedy, R.T., and Benner, S.A. (1999). Quantitative analysis of receptors for adenosine nucleotides obtained via in vitro selection from a library incorporating a cationic nucleotide analog. *J. Am. Chem. Soc.* **121**, 9781–9789.
42. Soukup, G.A., Emilsson, G.A., and Breaker, R.R. (2000). Altering molecular recognition of RNA aptamers by allosteric selection. *J. Mol. Biol.* **298**, 623–632.
43. Jose, A.M., Soukup, G.A., and Breaker, R.R. (2001). Cooperative binding of effectors by an allosteric ribozyme. *Nucleic Acids Res.* **29**, 1631–1637.
44. Huang, X., Holden, H.M., and Rauschel, F.M. (2001). Channeling of substrates and intermediates in enzyme-catalyzed reactions. *Annu. Rev. Biochem.* **70**, 149–180.
45. Bartel, D.P., Zapp, M.L., Green, M.R., and Szostak, J.W. (1991). HIV-1 Rev regulation involves recognition of non-Watson-Crick base pairs in viral RNA. *Cell* **67**, 529–536.
46. Baskerville, S., Zapp, M., and Ellington, A.D. (1995). High-resolution mapping of the human T-cell leukemia virus type 1 Rex-binding element by in vitro selection. *J. Virol.* **69**, 7559–7569.
47. Eklund, E.H., and Bartel, D.P. (1995). The secondary structure and sequence optimization of an RNA ligase ribozyme. *Nucleic Acids Res.* **23**, 3231–3238.
48. Robertson, M.P., Hesselberth, J.R., and Ellington, A.D. (2001). Optimization and optimality of a short ribozyme ligase that joins non-Watson-Crick base pairings. *RNA* **7**, 513–523.
49. Cherry, J.R., Lamsa, M.H., Schneider, P., Vind, J., Svendsen, A., Jones, A., and Pedersen, A.H. (1999). Directed evolution of a fungal peroxidase. *Nat. Biotechnol.* **17**, 379–384.
50. Gonzalez-Blasco, G., Sanz-Aparicio, J., Gonzalez, B., Hermoso, J.A., and Polaina, J. (2000). Directed evolution of beta-glucosidase A from *Paenibacillus polymyxa* to thermal resistance. *J. Biol. Chem.* **275**, 13708–13712.
51. Nielsen, J.E., Borchert, T.V., and Vriend, G. (2001). The determinants of alpha-amylase pH-activity profiles. *Protein Eng.* **14**, 505–512.
52. Pan, T. (1997). Novel and variant ribozymes obtained through in vitro selection. *Curr. Opin. Chem. Biol.* **1**, 17–25.
53. Wilson, D.S., and Szostak, J.W. (1999). In vitro selection of functional nucleic acids. *Annu. Rev. Biochem.* **68**, 611–647.
54. Ellington, A.D., and Robertson, M.P. (1999). Ribozyme Selection. In *Comprehensive Natural Products Chemistry*, D. Barton, K. Nakanishi, and O. Meth-Cohn, eds. (New York: Elsevier), pp. 115–148.
55. Jaschke, A., and Seelig, B. (2000). Evolution of DNA and RNA as catalysts for chemical reactions. *Curr. Opin. Chem. Biol.* **4**, 257–262.
56. Hesselberth, J., Robertson, M.P., Jhaveri, S., and Ellington, A.D. (2000). In vitro selection of nucleic acids for diagnostic applications. *J. Biotechnol.* **74**, 15–25.
57. Seetharaman, S., Zivarts, M., Sudarsan, N., and Breaker, R.R. (2001). Immobilized RNA switches for the analysis of complex chemical and biological mixtures. *Nat. Biotechnol.* **19**, 336–341.
58. Marshall, K.A., and Ellington, A.D. (1999). Training ribozymes to switch. *Nat. Struct. Biol.* **6**, 992–994.